

# Z-gradient coil optimisation in presence of time-varying eddy currents

A. Trakic<sup>1</sup>, F. Liu<sup>1</sup>, H. Sanchez Lopez<sup>1</sup>, H. Wang<sup>1</sup>, and S. Crozier<sup>1</sup>

<sup>1</sup>The School of Information Technology and Electrical Engineering, The University of Queensland, Brisbane, Queensland, Australia

**Synopsis:** The switching of magnetic field gradient coils in MRI inevitably induces transient eddy currents in conducting system components such as the cryostat vessel [1]. These eddy currents generate secondary magnetic fields that degrade the spatial and temporal performance of the gradient coil. This theoretical study shows that by incorporating the eddy current effects into the coil optimisation process, it is possible to modify a gradient coil design so that the fields created by the coil and the eddy currents combine together to generate a spatially homogeneous gradient, which follows the desired temporal variation. Shielded and unshielded longitudinal gradient coils are used to exemplify this novel approach.

**Method:** A shielded/unshielded z-gradient coil is commonly optimised to generate a homogeneous magnetic field gradient (to 5%pp) that follows a pure trapezoidal temporal variation [2]. However, when this coil is situated inside a realistic cryostat vessel and the coil current is pulsed trapezoidally, the resulting primary magnetic field induces transient eddy currents in the conductor, which in turn generate secondary magnetic fields in the imaging volume, thus spatially and temporally distorting the desired gradient. To compensate for these disturbances in this method, both the gradient coil current distribution and temporal variation (pre-emphasis excitation) are optimised to control the eddy current contributions in the imaging volume. In this way, the eddy current effects are strictly taken into account during gradient design procedure. The pre-emphasis can be achieved with a series of exponential functions. In the calculations, a number  $N$  of temporal sample points equally spaced in time is used to discretise the switching sequence (i.e. the pre-emphasis). The  $n^{\text{th}}$ -temporal sample point (TSP) can be found at time  $t_n = n\Delta\tau$ . At every TSP, the primary and secondary axial magnetic field is computed at  $M$  spatial sample points evenly distributed on the upper quarter of the DSV periphery:

$$z_m = R_z - \Delta Z(m-1) \quad r_m = R_r \sin(a \cos(z_m / R_z)) \quad m \in \{1..M\}$$

where  $r_m$  and  $z_m$  denote the radial and axial two-dimensional axial-symmetric cylindrical coordinates of the spatial sample points (SSP) in [m], respectively;  $\Delta Z$  is the fixed axial distance between adjacent sample points in [m],  $R_r$  and  $R_z$  are the radial and axial DSV semi-axes in [m] and  $m$  is the index of the SSP. The primary magnetic field due to the gradient coil is computed with the Biot-Savart method, while the secondary magnetic field due to the eddy currents is calculated using the TFSF-FDTD method described in our companion paper. The total time-varying axial magnetic field is:  $B_z^{\text{tot}}(r_m, z_m, t_n) = B_z^p(r_m, z_m, t_n) + B_z^s(r_m, z_m, t_n) \quad m \in \{1..M-1\}$ . The magnetic field gradient is expressed by the following difference equation:

$$G_z^{\text{tot}}(r_m, z_m, t_n) = \frac{B_z^{\text{tot}}(r_{m+1}, z_m, t_n) - B_z^{\text{tot}}(r_m, z_m, t_n)}{\Delta Z} \quad m \in \{1..M-1\}$$

For every TSP, the maximum and minimum total magnetic field gradient value is computed based on the dataset of total gradient values on  $M$  SSP:

$$G_{z,\text{max}}^{\text{tot}}(t_n) = \max(G_z^{\text{tot}}(r_m, z_m, t_n)) \quad \wedge \quad G_{z,\text{min}}^{\text{tot}}(t_n) = \min(G_z^{\text{tot}}(r_m, z_m, t_n))$$

Here  $G_{z,\text{max}}^{\text{tot}}(t_n)$  and  $G_{z,\text{min}}^{\text{tot}}(t_n)$  signify the maximum and minimum total gradient field waveform traces over time, respectively. These waveforms contain the eddy current induced distortions. The closest desired gradient is then given by:  $G_{z,\text{avg}}^{\text{tot}}(t_n) = 0.5(\max(G_{z,\text{max}}^{\text{tot}}(t_n)) + \max(G_{z,\text{min}}^{\text{tot}}(t_n)))$ ;  $G_{z,\text{CD}}(t_n) = G_{z,\text{avg}}^{\text{tot}}(t_n) \cdot \Xi(t_n)$

The objective is to minimize the difference between  $G_{z,\text{CD}}(t_n)$  and the field extremes  $G_{z,\text{max}}^{\text{tot}}(t_n)$  and  $G_{z,\text{min}}^{\text{tot}}(t_n)$ . This is achieved by simultaneous optimisation of gradient coil current distribution and temporal pre-emphasis excitation. In this work we have successfully employed the non-linear Levenberg-Marquardt (LM) least-square optimisation algorithm to minimize the objective function:

$$\Psi = \sum_{n=1}^N \max \left[ \left( \frac{G_{z,\text{max}}^{\text{tot}}(t_n) - G_{z,\text{CD}}(t_n)}{G_{z,\text{CD}}(t_n)} \right)^2, \left( \frac{G_{z,\text{min}}^{\text{tot}}(t_n) - G_{z,\text{CD}}(t_n)}{G_{z,\text{CD}}(t_n)} \right)^2 \right]$$

The objective function  $\Psi$  is satisfied when its value at every temporal sample point is less than 5%pp (industry standard).

**Results and Discussion:** Table I lists the axial coordinates of the eddy current non-optimized and optimized gradient coils, indicating the changes in the axial positions required to accommodate the eddy current fields.

TABLE I - NON-OPTIMISED VS OPTIMISED UNSHIELDED Z-GRADIENTS

AXIAL COIL COORDINATES [+/- mm]							
Non-optimised	140	340	345	355	425	455	463 480 485 500
Optimised	140	335	340	353	425	494	463 480 485 500
Change	0	-5	-5	-2	0	+39	0 0 0 0

Figure 1 (top) illustrates the gradient uniformity deviations from the closest desired gradient over time for a) spatially and temporally non-optimised single layer longitudinal coil (Table I), b) spatially non-optimised gradient driven with optimal pre-emphasis and c) spatially optimised gradient driven with optimal pre-emphasis. The bottom plots of figure 1 are worst-case gradient uniformity snapshots within the working volume at 0.11ms after the start of the gradient waveform. According to the results, only the spatially and temporally optimised gradient produces the best coil performance.

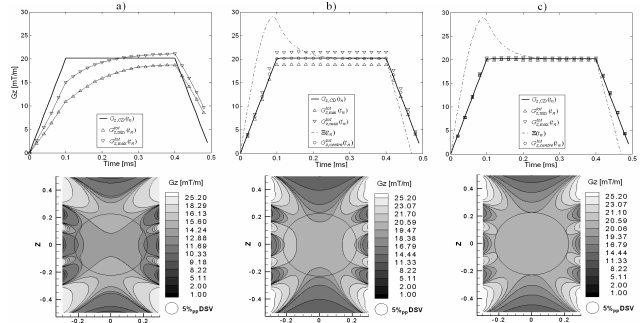


Figure 1 – Transient gradient due to the single-layer longitudinal gradient coil at 500A transport current and eddy currents induced in the cryostat vessel (top), and gradient uniformity snapshot at 0.11 ms after the start of the gradient waveform (bottom). The subplots illustrate: a) spatially and temporally non-optimised coil, b) spatially non-optimised coil driven with optimal pre-emphasis, c) spatially optimised gradient coil driven with optimal pre-emphasis.

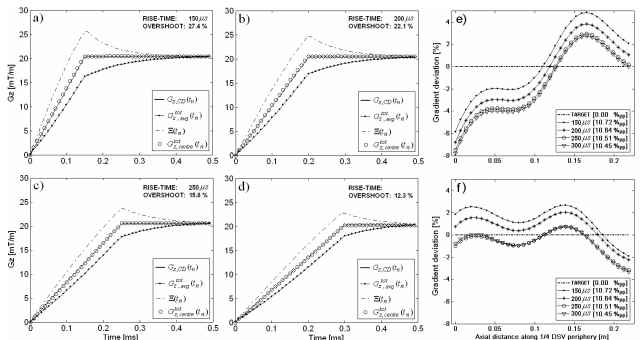


Figure 2 – a-d) Gradient field uniformity versus time analogous to figure 1 for various gradient rise times, e) spatially non-optimised coil (Table I) and optimal pre-emphasis and f) spatially and temporally optimised gradient coil.

Figure 2 shows that adjusting the optimal current distribution (wire positions) at the rise time of 100µs would require only a minor readjustment in the pre-emphasis excitation for slower rise times.

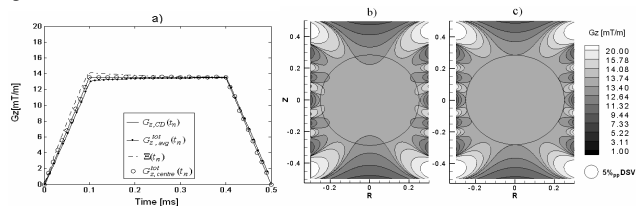


Figure 3 – a) Transient gradient due to the actively shielded longitudinal coil at 500A transport current and eddy currents induced in the cryostat vessel, b-c) gradient field snapshots in the imaging volume at 0.11ms after the start of the gradient waveform; results illustrated in b) and c) are obtained without and with spatial optimisation respectively.

TABLE II - NON-OPTIMISED VS OPTIMISED ACTIVELY SHIELDED Z-GRADIENTS

Layer	AXIAL COIL COORDINATES [+/- mm]															
	1 <sup>st</sup>	Non-optimised	98	196	221	282	362	395	411	419	452	455	458	461	464	467
	Change	-3	-3	+2	+4	0	-3	-1	-4	-7	-6	-3	-2	0	+5	-1
2 <sup>nd</sup>	Non-optimised	115	198	269	341	380	416	434	434	463	482	526				
	Change	-3	+2	+9	-2	0	-3	-1	+4	+1	+2					

Figure 3 and Table II illustrate analogous results for an actively-shielded gradient coil/ cryostat vessel model.

**Conclusion:** By incorporating transient eddy currents induced in MRI conductors in the gradient coil design process, good gradient uniformities with desired temporal variation can be obtained.

**Acknowledgements:** Financial support from the Australian Research Council is gratefully acknowledged.

## References:

- [1] E.A. Badaea and O. Craiu, *IEEE Trans. Magn.*, **33** (2): 1330-1333, 1997.
- [2] R. Turner, *Magnetic Resonance Imaging*, **11**: 903-920, 1993.